

Anticancer Effect of Dihydroartemisinin (DHA) in a Pancreatic Tumor Model Evaluated by Conventional Methods and Optical Imaging

WINN AUNG, CHIZURU SOGAWA, TAKAKO FURUKAWA and TSUNEO SAGA

*Diagnostic Imaging Program, Molecular Imaging Center,
National Institute of Radiological Sciences, Chiba, Japan*

Abstract. *Background: Dihydroartemisinin (DHA) inhibits the growth of certain cancer cells and xenograft tumors. Further understanding of the molecular mechanisms and genetic participants that govern the antineoplastic effects of DHA is necessary. The anticancer effects of DHA and its underlying mechanisms in pancreatic cancer and the efficacy in animal models by noninvasive optical imaging were evaluated. Materials and Methods: Combined with cell/tumor growth assays, flow cytometric analysis, and Hoechst staining, the effect of DHA was investigated using the pancreatic cancer cell line BxPc3-RFP stably expressing red fluorescence protein and in vitro/in vivo optical imaging. Proteins that regulate proliferation (PCNA), apoptosis (Bax and Bcl-2), and angiogenesis (vascular endothelial growth factor (VEGF)) were evaluated in cell and tumor samples by Western blotting and immunohistochemical analyses. Results: DHA inhibited the proliferation and viability of cells in a dose-dependent manner and induced apoptosis. We observed down-regulation of PCNA and Bcl-2, and up-regulation of Bax. VEGF was down-regulated by DHA in cells under normoxic, but not hypoxic, conditions. Fluorescence intensity emitted from cells and tumors correlated linearly with cell count and tumor burden, respectively. Conclusion: DHA inhibits cell and tumor growth by interfering with cell proliferation and inducing apoptosis. The antiangiogenic effect of DHA appears to be a complicated process. Optical imaging supports the real-time assessment of DHA efficacy in a preclinical model and comprehensive analysis substantiates that DHA is a potential candidate for pancreatic cancer therapy.*

Correspondence to: Winn Aung, Diagnostic Imaging Program, Molecular Imaging Center, National Institute of Radiological Sciences, Anagawa 4-9-1, Inage-ku, Chiba 263-8555, Japan. Tel: +81 433823706, Fax: +81 432060818, e-mail: winn@nirs.go.jp

Key Words: Dihydroartemisinin, pancreatic cancer, cell proliferation, apoptosis, angiogenesis, optical imaging.

Adenocarcinoma of the pancreas has the worst prognosis among solid tumors and there has been limited progress in its management over recent decades. Although chemotherapy is used at any stage of pancreatic cancer as adjuvant or neoadjuvant treatment, the resistance of this disease to chemotherapy restricts successful treatment. Thus, discovering new chemotherapeutic drugs and treatment strategies is a challenging issue for the management of pancreatic cancer.

Some natural plant compounds provide a potential source of chemotherapeutic agents and affect various cancer entities. One such promising natural compound is artemisinin, isolated from a Chinese herb *Artemisia annua* (commonly known as qinghaosu), which has been used by Chinese traditional medicine practitioners for at least 2,000 years to treat fever (1). Artemisinin is now recognized as a potent antimalarial drug by the World Health Organization. In recent years, evidence has emerged that artemisinin and some of its active derivatives inhibit the growth of human cancer cells (2-4). Dihydroartemisinin (DHA), a semisynthetic derivative and active metabolite of artemisinin, has inhibitory effects on the growth of certain cancer cells in culture and cell line-derived tumors in nude mouse xenografts (5-8). The molecular mechanisms and the genetic participants governing the antineoplastic effects of DHA are somewhat known but are not conclusive and a greater understanding is therefore necessary.

In the process of drug development, strategies using various imaging techniques, such as optical imaging, magnetic resonance imaging, computed tomography, positron-emission tomography, and ultrasonography, are being designed to reveal the response to therapy noninvasively. Among these, the faster, high-throughput, and more cost-effective imaging methods that can be tested in preclinical models are becoming primary methods for assessing efficacy. To obtain the most information regarding the efficacy of a therapeutic option in animal models of cancer, longitudinal monitoring of tumor progression and regression in a single animal throughout the entire course of

treatment in real time is worthwhile. *In vivo* optical imaging is a suitable tool for real-time qualitative and quantitative characterization of the pharmacologic effects of a drug on tumor growth.

In this study, we examined the potential mechanisms of action of the anticancer drug candidate DHA in relation to antiproliferative and antiangiogenic effects and induction of apoptosis, and noninvasively assessed and evaluated the therapeutic efficacy of DHA using an optical imaging system. For both purposes, we used the pancreatic cancer cell line BxPc3-RFP, which stably expresses the red fluorescence protein (RFP) reporter gene, and an optical imaging tool in both *in vitro* and *in vivo* settings.

Materials and Methods

Cell culture and reagents. The human pancreatic cancer cell line BxPc3-RFP expressing RFP (DsRed2) was purchased from Anticancer (San Diego, CA, USA). Cells were cultivated at 37°C in a humidified atmosphere containing 5% CO₂ in RPMI-1640 medium (Sigma, St. Louis, MO, USA) supplemented with 10% fetal bovine serum (Nichirei Biosciences, Tokyo, Japan), 100 U/ml penicillin-G sodium, and 100 mg/ml streptomycin sulfate (Invitrogen, Carlsbad, CA, USA). DHA and Hoechst 33342 were purchased from Tokyo Chemical Industry (Tokyo, Japan) and Sigma, respectively.

***In vitro* fluorescence imaging and cell growth assay.** BxPc3-RFP cells (3.5×10^4 cells/well) were seeded in poly D-lysine-coated black, μ Clear 96-well plates (Greiner Bio-One, Frickenhausen, Germany) with 0.2 ml medium. After 24 h, the cells were treated with dimethyl sulfoxide (DMSO) (control) or different concentrations (2.5, 10, 40, or 80 μ M) of DHA dissolved in DMSO for 24, 48, and 72 h. At each time point, the fluorescence intensity emitted from cells was measured by the IVIS[®] lumina optical imaging system (Xenogen Corp., Alameda, CA, USA). The medium was changed to phosphate-buffered saline (PBS) just before measurement. A filter set for DsRed (excitation: 500-550 nm, emission: 575-650 nm, background excitation: 460-490 nm) and constant imaging parameters (exposure time: 2 s, binning: medium, lens aperture [f/stop]: 2, field of view: 10 cm, floor lamp level: high) were used. To obtain the autofluorescence-corrected images, the background filter image was subtracted from the primary excitation filter image using the Image Math tool and appropriate scaling factor, according to the Living Image[®] software version 2.6 (Xenogen Corp.) manual, and fluorescence intensity (FI) was measured as photons per second. After the measurement, the cells were trypsinized and viable cells showing trypan blue dye exclusion were counted with a hemocytometer.

Western blot analysis. Western blot analysis was performed to analyze proteins of interest from both cultured cells and tissue samples from the *in vivo* model (see below). Tumor cells were cultured in normoxic (20% O₂) or hypoxic conditions (1% O₂) for 18 h after adding different concentrations of DHA. Whole-cell lysates were prepared using RIPA buffer (Wako Pure Chemical Industries, Osaka, Japan). For preparing lysates from tissue samples, tumor tissue sections from control and DHA-treated mice were homogenized using tissue protein lysis reagent (CellLytic[™] MT) and protease inhibitor cocktail (Sigma-Aldrich) according to the

manufacturer's instructions. Total protein was measured using the DC protein assay kit (Bio-Rad Laboratories, Hercules, CA, USA). Protein (60 μ g) was separated on a 15% polyacrylamide gel (ATTO Corporation, Tokyo, Japan) and transferred to Immobilon-P membrane (Millipore, Billerica, MA, USA). The membrane was blocked with Block-Ace reagent (Dainippon Pharmaceutical, Osaka, Japan) at room temperature (RT) for 1 h and then incubated with primary antibody at RT for 1 h. The following primary antibodies were used: mouse anti-human PCNA (F-2) antibody, mouse anti-human BAX (2D2) antibody, mouse anti-human BCL-2 (100) antibody, goat anti-human actin (C-11) antibody, rabbit anti-human VEGF (A-20) antibody (Santa Cruz Biotechnology, Santa Cruz, CA, USA), and mouse anti-human HIF-1 α (BD Transduction Laboratories, Franklin Lakes, NJ, USA). After incubating with respective primary antibody, the membrane was washed 3 times with Tris-buffered saline (TBS) containing 0.05% Tween 20, and incubated with appropriate horseradish peroxidase (HRP)-linked secondary antibody that was a donkey anti-rabbit IgG or sheep anti-mouse IgG (GE Healthcare, Little Chalfont, UK), or donkey anti-goat IgG (Santa Cruz Biotechnology). Immunoreactive bands were visualized using the Enhanced Chemiluminescence Plus Western blotting detection system (GE Healthcare) and images were obtained by Chemi-Smart 5000 (Vilber Lourmat, Marne-la-Vallée, France). Membranes were stripped and incubated with each dedicated antibody to detect the level of different proteins in the same membrane.

Flow cytometry and quantification of cellular apoptosis. Apoptotic cells were detected and quantified by flow cytometric analysis using the Guava PCA and Guava Nexin Assay (Guava Technologies, Hayward, CA, USA). The protocol was performed according to the manufacturer's instructions. Forty-eight hours after DMSO (control) or different DHA concentration (2.5, 10, 40, or 80 μ M) treatments, cell suspensions were incubated with two staining reagent mixtures to distinguish the apoptotic and nonapoptotic cell populations. This assay utilizes annexin V-phycoerythrin to detect early apoptotic cells and 7-aminoactinomycin D (7-AAD) to detect late apoptotic and dead cells. The DHA dose-dependent apoptosis rate (%) was calculated by summation of early and late apoptotic cells. The experiments were repeated twice.

Detecting morphological change of apoptotic cells. BxPc3-RFP cells were seeded in 35-mm glass-bottom dishes (1×10^5 /dish) in medium with DMSO (control) or different concentrations (2.5, 10, or 40 μ M) of DHA. After 24 h, the media were discarded and attached cells were washed with PBS and fixed in 4% paraformaldehyde for 10 min at RT. Fixed cells were stained with Hoechst reagent (1 μ g/ml) at RT for 10 min, washed with PBS, and examined with an Olympus FV1000 confocal laser microscope (Olympus, Tokyo, Japan) with respective excitation and emission filters for Hoechst dye.

Development of animal tumor model. All animal model experiments were carried out in accordance with the guidelines for animal experimentation determined by the Institutional Animal Care and Use Committee of the National Institutes of Radiological Sciences. BxPc3-RFP cells (5×10^6 in 100 ml culture medium) were mixed with 50 ml of phenol red-free BD Matrigel Matrix (BD Biosciences, Bedford, MA, USA) and subcutaneously inoculated into the flank of nude mice (8-week-old females, BALB/cA Jcl-nu/nu mice; CLEA, Japan) under anesthesia (inhalation of 2.5% isoflurane).

In vivo DHA treatment protocol and tumor growth study. Mice were divided into two groups when their tumor masses had reached approximately 70-110 mm³ to compare the growth rate of tumors in mice receiving DHA or control treatment. The treatment group and control group received 3 d on and 1 d off intraperitoneal injections of 25 mg/kg DHA in 50 µl DMSO and 50 µl DMSO, respectively, for 4 weeks. Gross appearance and tumor growth were monitored by caliper measurements every 3-4 d. Tumor volume was estimated as $V \text{ (mm}^3\text{)} = \text{length (mm)} \times (\text{width [mm]})^2 / 2$. Relative tumor volume was calculated as the volume at the indicated day divided by the volume at the starting day of treatment. Each mouse was weighed every 3-4 d.

In vivo fluorescence imaging of tumor. For fluorescence imaging of *in vivo* tumors, mice bearing xenograft tumors were anesthetized by inhalation of 2.5% isoflurane and images were acquired using the same settings described for *in vitro* fluorescence imaging with the exception that the exposure time was 1 s, the lens aperture (*f*/stop) was 4, and the field of view was 12.5 cm. This procedure was performed every 3-4 d. For quantitative analysis, regions of interest were encircled over the tumors by auto contour mode and FI was measured as photons per second with the above-mentioned software. Relative FI was calculated as FI at the indicated day divided by FI at the starting day of treatment.

Immunohistochemical analysis. When the treatment protocol was finished, the animals were sacrificed and tumor specimens were fixed in 4% paraformaldehyde followed by dehydration and paraffin embedding. For immunohistochemical analysis, specimens were sectioned (4 µm thickness) and mounted on a glass slide. Tissue sections were subsequently deparaffinized and rehydrated with graded ethanol. For antigen retrieval, the slides were incubated in sodium citrate buffer (pH 6) for 20 min at 95°C. Endogenous peroxidase activity was blocked with 0.3% hydrogen peroxide in methanol for 10 min at RT. Each section was washed 3 times for 5 min with TBS and incubated with nonspecific blocking reagent (DAKO X0909; DAKO, Carpinteria, CA, USA) for 10 min at RT. Sections were incubated with the same primary antibodies as used in Western blotting analysis with the exception that mouse anti-mouse Bax (B-9) antibody (Santa Cruz Biotechnology) and mouse anti-human HIF-1α (MILLIPORE, Temecula, CA, USA) were used for Bax and HIF-1α, respectively. The reaction with the primary antibodies was performed for 1 h at RT. After the incubation with the primary antibodies, each section was washed 3 times for 5 min with TBS at RT and then incubated with secondary antibody labeled with peroxidase (EnVision+ System, mouse HRP or Rabbit HRP, DAKO K4000 and K4002; DAKO) for 1 h at RT. The sections were washed in distilled water, stained with diaminobenzidine (DAKO K3465; DAKO) for 2 min at RT, and washed in distilled water. Counterstaining was carried out with hematoxylin.

Statistical analysis. Significant differences between groups were determined by Student's *t*-test. *P*-values less than 0.05 were considered significant.

Results

Effect of DHA on cell growth and viability of the BxPc3-RFP pancreatic cancer cell line. DHA inhibited the growth of BxPc3-RFP cells in a dose-dependent manner. A decrease in FI emitted from the cultured cells was observed in the *in vitro* fluorescence images at 24, 48, and 72 h (Figure 1A). The

quantified FI decreased with increasing doses of DHA (Figure 1B). In addition, trypan blue dye exclusion showed a dose-dependent decrease in viable cell count after DHA treatment (Figure 1C). The viable cell numbers from each cultured well strongly correlated with the respective quantified FI ($R^2=0.997$, 0.979, and 0.913 for 24, 48, and 72 h, respectively) (Figure 1D).

DHA induces cellular apoptosis and morphological changes. Apoptotic cells were detected and quantified in DHA-treated and control cells by using flow cytometry (Figure 2A). The sum of early apoptotic cells and late apoptotic cells (including dead cells) increased in a DHA dose-dependent manner (Figure 2B). Consistent with this finding, Hoechst apoptosis-detection staining demonstrated augmented chromatin condensation and nuclear fragmentation in the DHA-treated cells compared with the untreated cells under a fluorescence microscope (Figure 2C).

Effect of DHA on regulation of cell proliferation-, apoptosis- and angiogenesis-related protein expression in cells. Key regulatory proteins of cell proliferation, apoptosis, and angiogenesis were examined by Western blotting to reveal the molecular pathways involved in the DHA-induced effect (Figure 3). After exposure to different concentrations of DHA, tumor cells were cultured in normoxic or hypoxic conditions for 18 h. Expression of proliferating cell nuclear antigen (PCNA), which is synthesized in the early G₁ and S phases of the cell cycle, was down-regulated in both conditions and this down-regulation was DHA dose-dependent.

After DHA treatment, expression of the proapoptotic protein Bax was increased in both conditions in a dose-dependent fashion. In contrast, the antiapoptotic protein Bcl-2 was down-regulated.

To explore another antitumorigenic effect of DHA, we investigated expression of VEGF, which is a potent angiogenic factor and is a down-stream gene of HIF-1α. HIF-1α expression was not detected in normoxic conditions but VEGF expression was detected and was down-regulated by DHA in a dose-dependent manner. In hypoxic conditions, HIF-1α expression was detected and down-regulated by DHA treatment. However, no obvious change was noted in VEGF expression in cells treated with DHA under hypoxic conditions.

Effect of DHA on tumor growth in nude mice. Tumors from DHA-treated mice showed significant tumor growth delay ($p<0.05$) compared to the control group (Figure 4A). The average body weight of DHA-treated and control mice did not differ throughout the experiment (data not shown).

Correlation of quantified tumor photon emission with geometric tumor volume. Longitudinal optical imaging was undertaken in tumor-bearing mice that did or did not receive treatment. The FI emitted from tumors was monitored and quantified for comparison between the groups (Figure 4C).

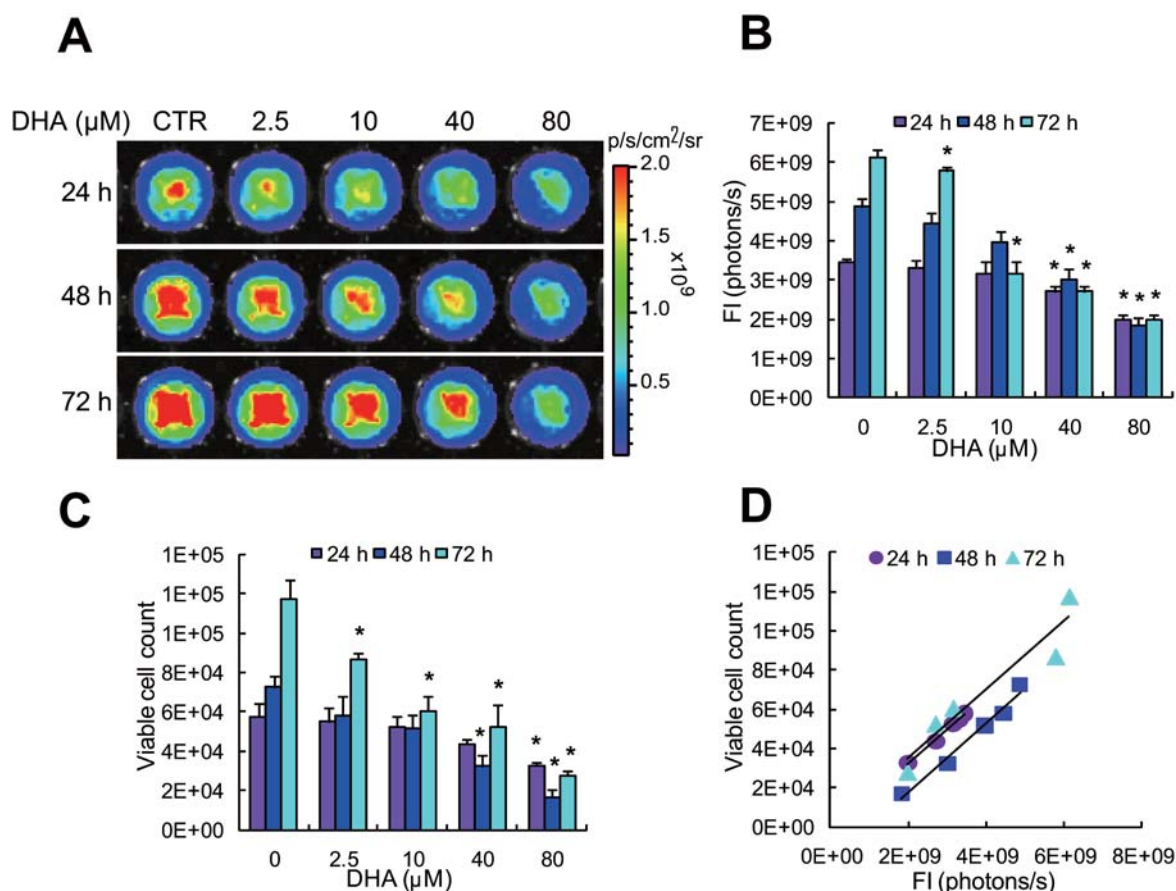


Figure 1. Effect of DHA on cell growth and viability of human pancreatic cancer BxPc3-RFP cells. A: Fluorescence image of cells seeded in 96-well plates after incubation with DHA (2.5, 10, 40, or 80 μM) or dimethyl sulfoxide (DMSO) (control) for 24, 48, and 72 h. B: Quantified fluorescence intensity (FI) decreased in a DHA dose-dependent manner. Data represent the mean FI \pm SD, (n=3), *p<0.05 compared to the control. C: Cell viability as determined with trypan blue dye exclusion declined in a DHA dose-dependent manner. Data represent mean viable cell count \pm SD, (n=3), *p<0.05 compared to the control. D: Quantified FI showed a strong linear correlation with viable cell number. R2 indicates the correlation coefficient, which was 0.997, 0.979, and 0.913 for 24, 48, and 72 h, respectively.

Relative FI was comparatively lower in the treatment group, although this difference was not statistically significant (Figure 4B). Nevertheless, we observed a linear correlation between relative FI and relative tumor volume. The correlation coefficient R2 was 0.816 and p value was less than 0.05 in both groups (Figure 4D).

DHA modulation of expression of proteins associated with cell proliferation, apoptosis, and angiogenesis in the in vivo tumors.

To determine whether the regression of tumor growth by DHA is followed by DHA-induced changes in expression of proliferation-, apoptosis- and angiogenesis-related key proteins *in vivo*, tumor tissue samples from DHA-treated and control mice were subjected to Western blot analysis. *In vivo* protein expression showed down-regulation of PcnA, up-regulation of Bax, down-regulation of Bcl-2, down-regulation of Hif-1 α , and no obvious change in Vegf (Figure 5A). Immunohistochemical

staining of tumor sections showed decreased PcnA-positive cells in samples from DHA-treated compared with control mice, consistent with protein expression profiles from Western analysis. Bax-positive cells increased and Bcl-2-positive cells decreased in samples from treated mice. Although HIF-1 α -expressing cells decreased with DHA treatment, there was a less obvious change in VEGF expression in tumor samples from treated mice (Figure 5B).

Discussion

Pancreatic cancer is a highly lethal and seldom curable tumor. Although surgical removal is the best option for treatment, curative surgery is feasible only in selected cases. Thus, chemotherapy remains important for palliative treatment. Gemcitabine is the current standard first-line drug and 5-fluorouracil (5-FU) is another commonly used drug. Other

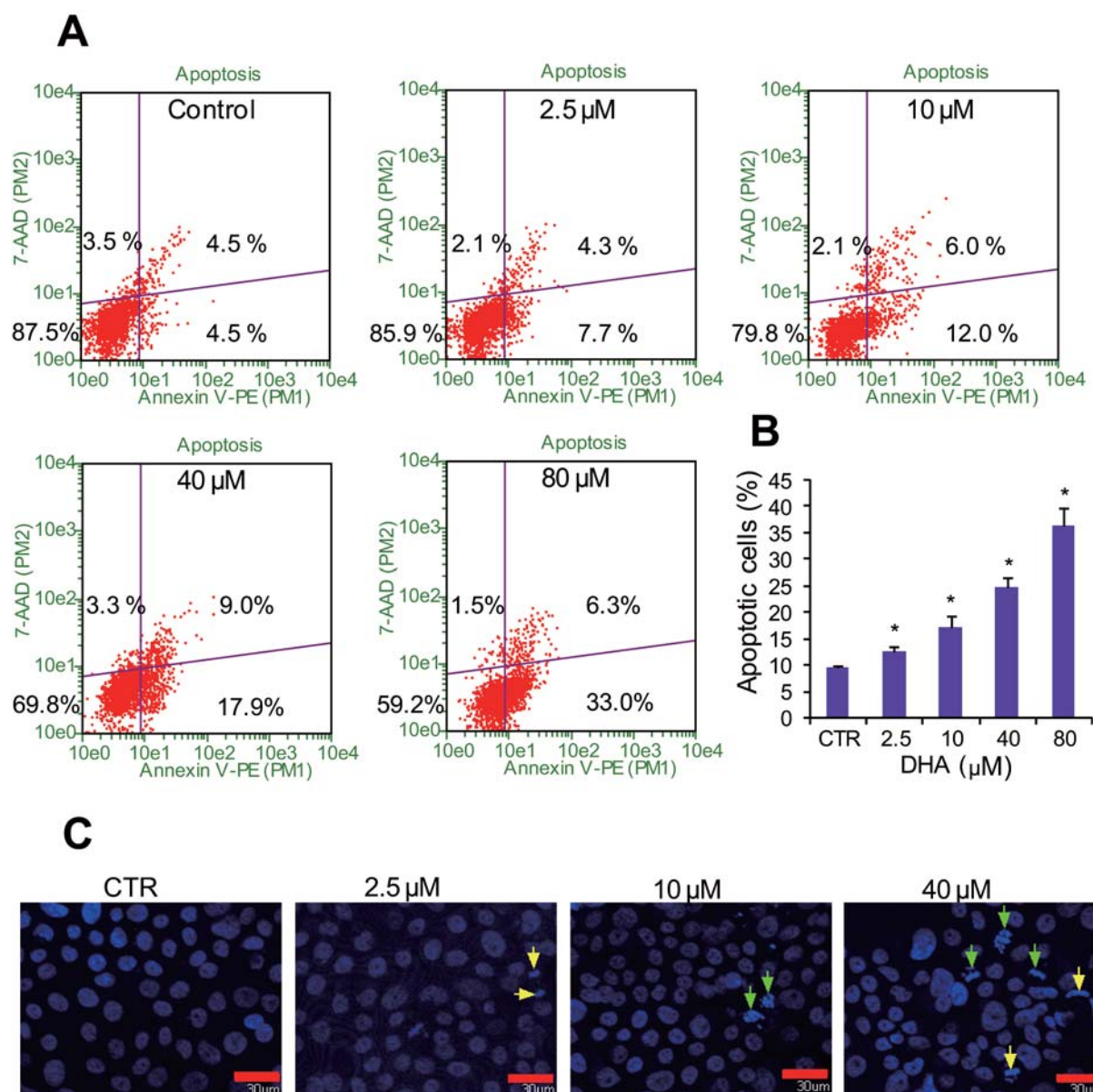


Figure 2. Effect of DHA on induction of apoptosis in BxPc3-RFP cells. **A:** After incubation with DMSO (control) or DHA (2.5, 10, 40, or 80 μM) for 48 h, flow cytometric analysis of apoptotic cells was performed using two staining reagent mixtures. Numbers in the corner of the lower left, lower right, and upper right of each graph indicate the percentage of live cells (annexin V-phycoerythrin negative/7-AAD negative), early apoptotic cells (annexin V-phycoerythrin positive/7-AAD negative), and late apoptotic and dead cells (annexin V-phycoerythrin positive/7-AAD positive), respectively. The representative results of three experiments are shown. **B:** Summation of early and late apoptotic cell percentage was defined as the apoptosis rate, which increased in a DHA dose-dependent manner. The data represent the mean \pm SD, ($n=3$), * $p<0.05$ compared to the control. **C:** The cells were treated with DHA for 24 h. Cell nuclear morphological changes were detected by Hoechst staining and fluorescence microscopy. Increasing doses of DHA induced greater chromatin condensation (yellow arrow) and nuclear fragmentation (green arrow) compared to untreated control cells (scale bar, 30 μm).

drugs such as cisplatin, irinotecan, paclitaxel, capecitabine, or oxaliplatin may be used in combination with gemcitabine or 5-FU. Resistance to chemotherapy is not uncommon and the development of novel therapeutic strategies and drugs are needed to combat pancreatic cancer. Among various anticancer candidates, the natural product artemisinin and its

derivatives, particularly DHA, have been studied for their cytotoxic effects on various cancer cell lines. Recently, a number of studies have reported that DHA inhibits the growth of several cancer cells lines and tumors such as leukemia (9, 10), glioma (11), fibrosarcoma (6), and breast (4), cervical (12), ovarian (13), lung (14), oral (15) and pancreatic cancer

(7). Several groups have shown that DHA-mediated cytotoxicity is tumor selective by comparing its effect on cancer cells and their counterpart normal cells (4, 8, 11, 12) or primary cells (11). The endoperoxide bridge of DHA is reportedly essential for its cytotoxicity because it reacts with intracellular ferrous iron to generate reactive oxygen species or carbon-centered radicals, leading to cytotoxicity (16, 17).

In general, a novel anticancer chemotherapeutic that can block cell proliferation, induce apoptosis, and inhibit angiogenesis is highly desirable. Chen *et al.* (7) investigated the anticancer effects of DHA and several of its underlying mechanisms, including antiproliferation and proapoptosis in pancreatic cancer *in vitro* and *in vivo*. In the present study, we examined the underlying mechanisms of the action of DHA by measuring several key regulating proteins of proliferation, apoptosis, and angiogenesis in cancer cells under normoxic and hypoxic conditions and *in vivo* samples using Western blotting and immunohistochemical methods. In addition, we corroborated the evidence of the effect of DHA in pancreatic cancer by measuring its effects using *in vitro/in vivo* optical imaging, together with conventional assays such as cell and tumor growth and apoptosis assays.

DHA-induced inhibition of proliferation in many types of cells has been previously shown (7, 11, 13, 15). Consistent with these reports, our results show that DHA effectively exerted cytotoxicity on pancreatic cancer cells. DHA inhibited cell proliferation and viability in a dose-dependent manner (Figure 1). PCNA is involved in the uncontrollable proliferation of cancer cells by assisting DNA replication and base excision repair (18). PCNA is synthesized during the early G₁ and S phases of the cell cycle. Thus, the expression of PCNA is correlated with the proliferative state of the cell (19) and is an accepted marker of cell proliferation. When PCNA is down-regulated by DHA, interruption of DNA replication and repair leads to inhibition of cell proliferation. We demonstrated that DHA mediated down-regulation of PCNA in pancreatic cancer cells after culture in both normoxic and hypoxic conditions by Western blotting (Figure 3). We included the hypoxic condition in our experimental protocol because the hypoxic microenvironment is an unavoidable consequence when tumors outgrow their supply of oxygen. In parallel with the findings of *in vitro* Western blotting experiments, down-regulation of PCNA expression and fewer PcnA-positive cells in xenograft tumors of DHA-treated mice were observed by Western blotting and immunohistochemical analysis of tumor samples, respectively (Figure 5).

In addition to the antiproliferative effect of DHA on pancreatic cancer cells, DHA was also shown to induce apoptosis in our study. This is consistent with studies depicting DHA-induced apoptosis *via* various signaling pathways, including the intrinsic and extrinsic apoptotic pathways (7, 8, 10, 13, 20, 21). Activation of the proapoptotic protein Bax is required for the initiation of the intrinsic apoptotic pathway,

whereas antiapoptotic proteins, such as Bcl-2, prevent apoptosis initiation by binding to and inactivating their proapoptotic counterparts (22). Our flow cytometric analysis and fluorescence microscopy after Hoechst staining revealed that DHA significantly induced apoptosis in a dose-dependent manner (Figure 2). Furthermore, with Western blotting analysis we confirmed that DHA not only up-regulates Bax expression but also down-regulates Bcl-2 expression in cells (Figure 3). Similarly, Western blot analysis of tumor tissue lysates and immunohistochemical staining of tissue samples showed down-regulation of Bcl-2 expression and up-regulation of Bax expression in DHA-treated tumors (Figure 5).

The tumor angiogenesis pathway may be a target for combating cancer. VEGF is presumably a principal mediator of angiogenesis in tumors and its transcription is regulated by HIF-1 α (23). Under hypoxic conditions, HIF-1 α is stabilized and activates target proteins such as VEGF (24). Although the effect of DHA on HIF-1 α /VEGF expression in pancreatic cancer cells has not been described, Haung *et al.* (11) reported that DHA inhibits HIF-1 α and VEGF expression in C6 glioma cells in both normoxic and hypoxic conditions. Lee *et al.* (9) showed that DHA down-regulates VEGF expression in chronic myeloid leukemia K562 cells, and Wu *et al.* (25) demonstrated that DHA down-regulates VEGF in multiple myeloma RPMI18226 cells under hypoxic conditions. In contrast, an interesting finding in our study is that DHA down-regulates VEGF expression in BxPc3-RFP cells under normoxic, but not under hypoxic, conditions. Although HIF-1 α expression was not observed in normoxia, its expression was detected and down-regulated by DHA in hypoxia (Figure 3). Western blot analysis of tissue extracts showed down-regulation of Hif-1 α and no obvious change in Vegf expression in tumors treated with DHA (Figure 5A). Immunohistochemical analysis also revealed that in spite of an observed decrease in Hif-1 α -expressing cells in tumor samples from DHA-treated mice, Vegf expression was less obviously changed (Figure 5B). On the basis of these results, there might be an HIF-1 α -independent regulatory pathway for VEGF expression, and the DHA-mediated suppressive effect was not sufficient to obtain Vegf down-regulation in a hypoxic environment for the cell line that we tested. Thus, angiogenesis regulation by DHA still needs to be explored. In addition, our study did not address possibilities such as down-regulation of VEGF receptors, interference with the binding of VEGF to its receptor, and the inhibition VEGF receptor tyrosine kinases as possible alternative mechanisms of DHA mediated-antiangiogenesis effects. Nonetheless, our *in vitro* and *in vivo* experiments collectively suggest that tumor regression was mainly due to the inhibition of proliferation as well as induction of apoptosis, and the antiangiogenic effect of DHA was less pronounced in our model.

In this study, we provide a traditional assessment and evaluation of the anticancer effect of DHA and demonstrate the applicable use of *in vivo* optical imaging to evaluate DHA

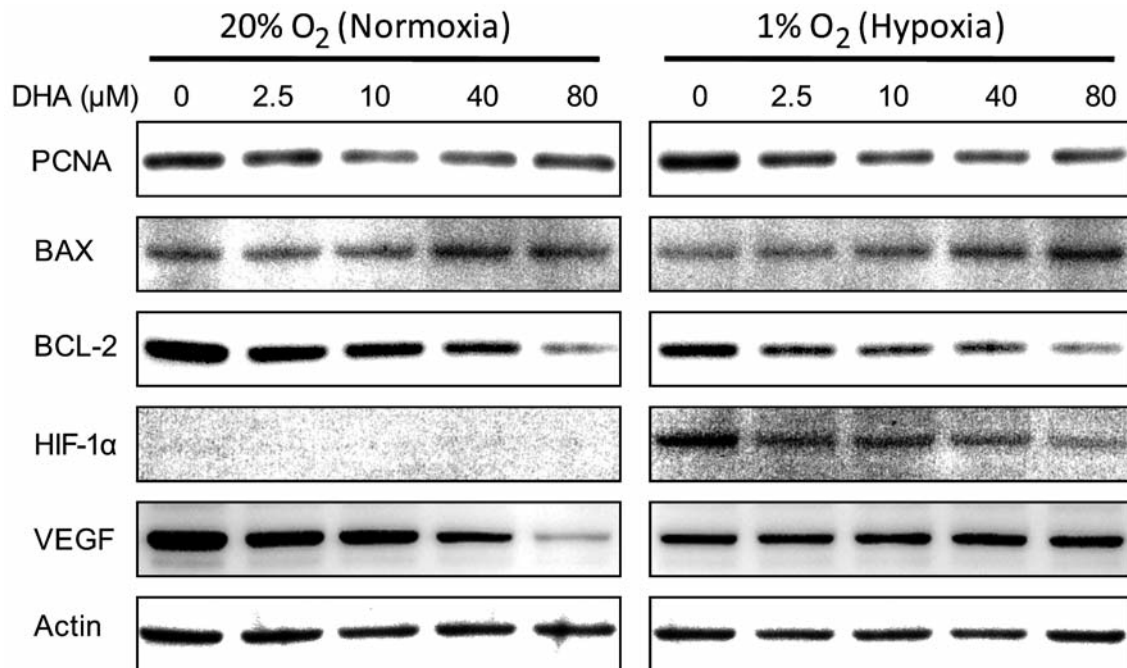


Figure 3. The effect of DHA on expression of key proliferation, apoptotic, and angiogenic proteins. Cells were treated with DHA (2.5, 10, 40, or 80 μM) or DMSO (control) and cultured in a prepared hypoxic (1% O_2) or normoxic (20% O_2) incubator for 18 h and cellular proteins were analysed by Western blotting. PCNA, a marker of proliferation, was down-regulated by DHA in a dose-dependent manner under both conditions. Expression of the proapoptotic protein BAX was up-regulated and that of antiapoptotic protein BCL-2 was down-regulated in both conditions and in a dose-dependent manner. Expression of the principle angiogenic factor VEGF was down-regulated in normoxic conditions, whereas no obvious change in VEGF expression was noted in DHA-treated cells under hypoxic conditions. Expression of the VEGF upstream gene, HIF-1 α , was down-regulated by DHA in hypoxic stress and was not detected under normoxic conditions. Actin served as a protein loading control. Representative Western blots from two experiments are shown.

therapy in a pancreatic xenograft for the first time. Among the different types of noninvasive imaging technologies, *in vivo* optical imaging has particular advantages such as low cost and rapid and easy operation. The use of an endogenously expressed green or red fluorescence-based optical imaging to measure tumor biometrics after antitumor therapy has been previously described in several pancreatic cancer models. Sun *et al.* determined the antitumor and antimetastatic efficacy of the camptothecin analog, DX-8951f (26), and Katz *et al.* reported the real-time visualization of tumor growth/metastasis and quantification of the therapeutic efficacy of the antimetabolite gemcitabine and topoisomerase inhibitor CPT-11 (27). However, to the best of our knowledge, no report has described the evaluation of the potential anticancer candidate DHA by fluorescence imaging.

In this study, we used the BxPC-3 cell line expressing the RFP fluorescent reporter gene to facilitate *in vitro* and *in vivo* monitoring of the tumor cell response to DHA. We showed that fluorescence emission allows monitoring and quantification of *in vitro* DHA-induced cancer cell growth inhibition (Figure 1). Moreover, we demonstrated that it was possible to visualize and measure the DHA effect on a preclinical tumor model externally

via fluorescence emission, which serves as a reliable surrogate for tumor biometric change because it correlated well with traditionally measured tumor volume (Figure 4D). This approach can provide real-time data that is directly relevant to tumor burden at multiple time points during treatment of the same animal. Rapid *in vitro* and *in vivo* whole-body imaging, along with the convenience of repeated measurements on cells and animals, can improve data collection, diminish stress to the animals, and expedite preclinical studies in new drug development.

In summary, DHA inhibits cell and tumor growth by modulating various tumor-suppressive pathways, such as inhibiting cell proliferation and inducing apoptosis through regulation of proliferation- and apoptosis-related proteins. In addition, we found that DHA down-regulates VEGF expression in tumor cells under normoxic conditions but not in a hypoxic environment. This indicates that effect of DHA on antiangiogenesis appears to be a complicated process that should be studied in further detail. In addition, we visualized and evaluated the anticancer effect of DHA *in vitro* and *in vivo* using pancreatic cancer cells that stably expressed the RFP reporter gene and optical imaging tools. This noninvasive, longitudinal imaging supported the convenient and reliable

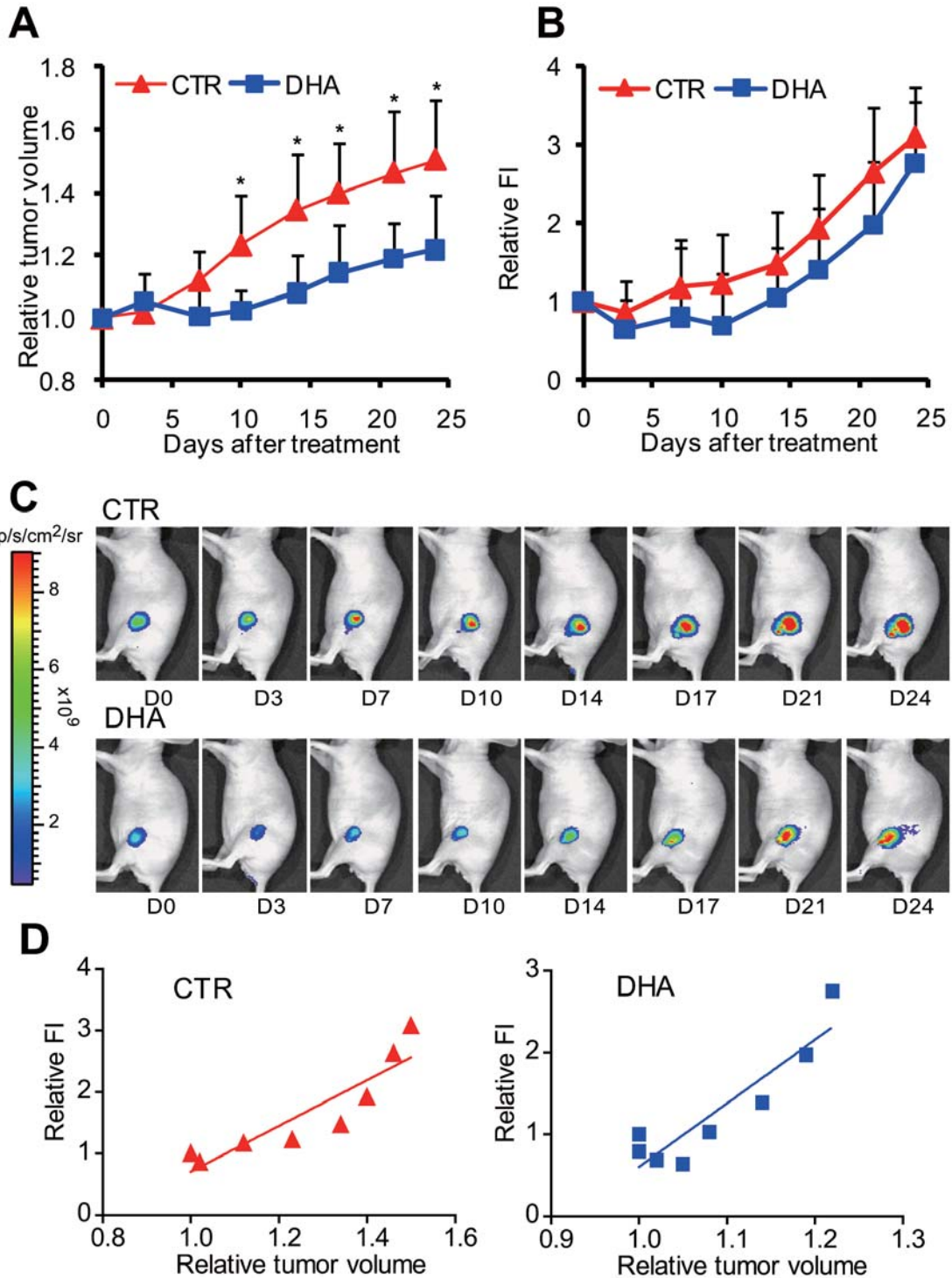


Figure 4. Effect of DHA on tumor growth in living mice. A: Traditional tumor volume measurement showed that tumors of DHA-treated mice had a significantly slower tumor growth rate than those of control mice. Tumor volume change is expressed as the relative tumor volume calculated as the volume at the indicated day divided by the volume at the starting day of treatment. The data represent the mean±SD, (n=6), *p<0.05 compared with the control. B: In vivo longitudinal optical imaging was performed, and quantified fluorescence intensities (FI) from tumors were compared between DHA-treated and untreated groups. Relative FI was calculated as FI at the indicated day divided by FI at the starting day of treatment. A comparatively lower relative FI was observed in the DHA-treated tumor than in controls. The data represent the mean±SD, (n=6). C: Representative images for temporal analysis of a tumor from a DHA-treated mouse (lower panel) and a control DMSO-treated mouse (upper panel) are shown. D: There was a linear correlation between relative FI and relative tumor volume. The correlation coefficient R² was 0.816 and p<0.05 for both DHA-treated and control groups.

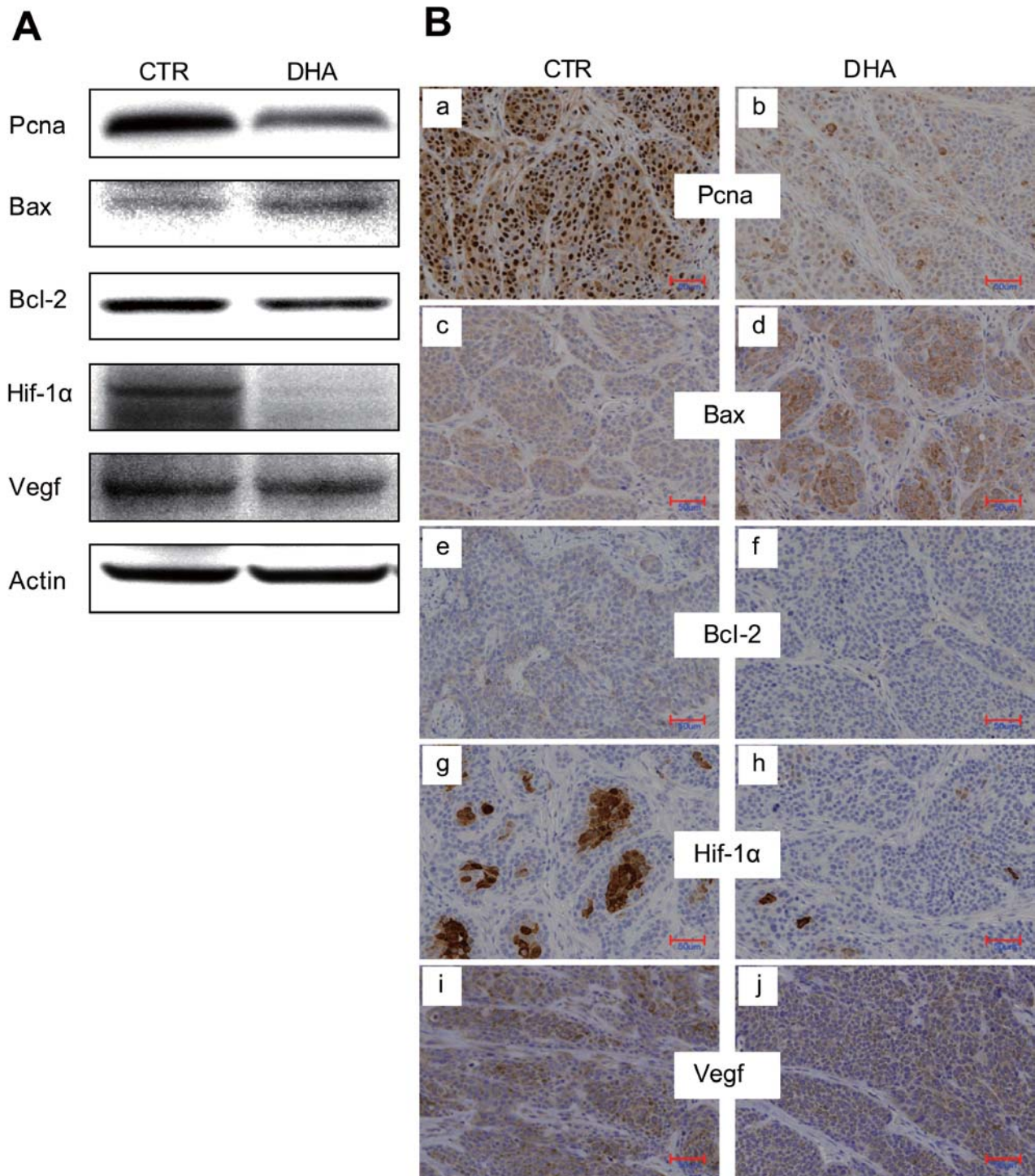


Figure 5. *In vivo* antitumor effect of DHA in xenograft tumors. A: Tumor tissue sections from mice receiving 3 d on and 1 d off intraperitoneal injection of DMSO (control), or DHA at a dose of 25 mg/kg for 4 weeks were homogenized and processed for Western blotting analysis to detect the expression of several key proteins associated with cell proliferation, apoptosis, and angiogenesis. Down-regulation of Pcna, up-regulation of Bax, down-regulation of Bcl-2, down-regulation of Hif-1 α , and no obvious change in Vegf expression were observed. Actin served as a protein loading control. B: Tumor sections from control (a, c, e, g, and i) and DHA-treated mice (b, d, f, h, and j) were prepared for immunohistochemical staining. Fewer Pcna-positive cells, Bcl2-positive cells, Hif-1 α -positive cells and more Bax-positive cells were observed in samples from DHA-treated mice compared to respective control samples. There was a subtle decrease of Vegf expression in samples from DHA-treated mice. Representative tumor sections are shown and each section was analyzed under a microscope at $\times 200$ magnification (scale bar, 50 μ m).

real-time assessment of DHA efficacy in a preclinical model. Taken together, our findings substantiate that DHA is a potential anticancer therapeutic for pancreatic cancer.

Conflict of Interest Statement

We declare that we have no conflict of interest.

Acknowledgements

We thank all members in our group for helpful discussions and suggestions, and the staff of the Laboratory of Animal Sciences, Section for Animal Management. This study was supported in part by a grant from the National Institute of Radiological Sciences

References

- Klayman DL: Qinghaosu (artemisinin): an antimalarial drug from China. *Science* 228: 1049-1045, 1985.
- Lai H and Singh NP: Selective cancer cell cytotoxicity from exposure to dihydroartemisinin and holotransferrin. *Cancer Lett* 91: 41-46, 1995.
- Efferth T, Dunstan H, Sauerbrey A, Miyachi H and Chitambar CR: The anti-malarial artesunate is also active against cancer. *Int J Oncol* 18: 767-773, 2001.
- Singh NP and Lai H: Selective toxicity of dihydroartemisinin and holotransferrin toward human breast cancer cells. *Life Sci* 70: 49-56, 2001.
- Chen HH, Zhou HJ and Fang X: Inhibition of human cancer cell line growth and human umbilical vein endothelial cell angiogenesis by artemisinin derivatives *in vitro*. *Pharmacol Res* 48: 231-236, 2003.
- Moore JC, Lai H, Li JR, Ren RL, McDougall JA, Singh NP and Chou CK: Oral administration of dihydroartemisinin and ferrous sulfate retarded implanted fibrosarcoma growth in the rat. *Cancer Lett* 98: 83-87, 1995.
- Chen H, Sun B, Pan S, Jiang H and Sun X: Dihydroartemisinin inhibits growth of pancreatic cancer cells *in vitro* and *in vivo*. *Anticancer Drugs* 20: 131-140, 2009.
- Hou J, Wang D, Zhang R and Wang H: Experimental therapy of hepatoma with artemisinin and its derivatives: *in vitro* and *in vivo* activity, chemosensitization, and mechanisms of action. *Clin Cancer Res* 14: 5519-5530, 2008.
- Lee J, Zhou HJ and Wu XH: Dihydroartemisinin downregulates vascular endothelial growth factor expression and induces apoptosis in chronic myeloid leukemia K562 cells. *Cancer Chemother Pharmacol* 57: 213-220, 2006.
- Zhou HJ, Wang Z and Li A: Dihydroartemisinin induces apoptosis in human leukemia cells HL60 *via* down-regulation of transferrin receptor expression. *Anticancer Drugs* 19: 247-255, 2008.
- Huang XJ, Ma ZQ, Zhang WP, Lu YB and Wei EQ: Dihydroartemisinin exerts cytotoxic effects and inhibits hypoxia inducible factor-1 α activation in C6 glioma cells. *J Pharm Pharmacol* 59: 849-856, 2007.
- Disbrow GL, Baege AC, Kierpiec KA, Yuan H, Centeno JA, Thibodeaux CA, Hartmann D and Schlegel R: Dihydroartemisinin is cytotoxic to papillomavirus-expressing epithelial cells *in vitro* and *in vivo*. *Cancer Res* 65: 10854-10861, 2005.
- Jiao Y, Ge CM, Meng QH, Cao JP, Tong J and Fan SJ: Dihydroartemisinin is an inhibitor of ovarian cancer cell growth. *Acta Pharmacol Sin* 28: 1045-1056, 2007.
- Lu YY, Chen TS, Qu JL, Pan WL, Sun L and Wei XB: Dihydroartemisinin (DHA) induces caspase-3-dependent apoptosis in human lung adenocarcinoma ASTC-a-1 cells. *J Biomed Sci* 16: 16, 2009.
- Nam W, Tak J, Ryu JK, Jung M, Yook JI, Kim HJ and Cha IH: Effects of artemisinin and its derivatives on growth inhibition and apoptosis of oral cancer cells. *Head Neck* 29: 335-340, 2007.
- Efferth T, Giaisi M, Merling A, Krammer PH and Li-Weber M: Artesunate induces ROS-mediated apoptosis in doxorubicin-resistant T leukemia cells. *PLoS ONE* 2: e693, 2007.
- Mercer AE, Maggs JL, Sun XM, Cohen GM, Chadwick J, O'Neill PM and Park BK: Evidence for the involvement of carbon-centered radicals in the induction of apoptotic cell death by artemisinin compounds. *J Biol Chem* 282: 9372-9382, 2007.
- Kelman Z: PCNA: structure, functions and interactions. *Oncogene* 14: 629-640, 1997.
- Tsurimoto T: PCNA, a multifunctional ring on DNA. *Biochim Biophys Acta* 1443: 23-39, 1998.
- Handrick R, Ontikatzte T, Bauer KD, Freier F, Rubel A, Durig J, Belka C and Jendrosseck V: Dihydroartemisinin induces apoptosis by a Bak-dependent intrinsic pathway. *Mol Cancer Ther* 9: 2497-2510, 2010.
- He Q, Shi J, Shen XL, An J, Sun H, Wang L, Hu YJ, Sun Q, Fu LC, Sheikh MS and Huang Y: Dihydroartemisinin up-regulates death receptor 5 expression and cooperates with TRAIL to induce apoptosis in human prostate cancer cells. *Cancer Biol Ther* 9: 819-824, 2010.
- Youle RJ and Strasser A: The BCL-2 protein family: opposing activities that mediate cell death. *Nat Rev Mol Cell Biol* 9: 47-59, 2008.
- Jensen RL, Ragel BT, Whang K and Gillespie D: Inhibition of hypoxia inducible factor-1 α (HIF-1 α) decreases vascular endothelial growth factor (VEGF) secretion and tumor growth in malignant gliomas. *J Neurooncol* 78: 233-247, 2006.
- Damert A, Machein M, Breier G, Fujita MQ, Hanahan D, Risau W and Plate KH: Up-regulation of vascular endothelial growth factor expression in a rat glioma is conferred by two distinct hypoxia-driven mechanisms. *Cancer Res* 57: 3860-3864, 1997.
- Wu XH, Zhou HJ and Lee J: Dihydroartemisinin inhibits angiogenesis induced by multiple myeloma RPMI8226 cells under hypoxic conditions *via* down-regulation of vascular endothelial growth factor expression and suppression of vascular endothelial growth factor secretion. *Anticancer Drugs* 17: 839-848, 2006.
- Sun FX, Tohgo A, Bouvet M, Yagi S, Nassirpour R, Moossa AR and Hoffman RM: Efficacy of camptothecin analog DX-8951f (exatecan mesylate) on human pancreatic cancer in an orthotopic metastatic model. *Cancer Res* 63: 80-85, 2003.
- Katz MH, Takimoto S, Spivack D, Moossa AR, Hoffman RM and Bouvet M: A novel red fluorescent protein orthotopic pancreatic cancer model for the preclinical evaluation of chemotherapeutics. *J Surg Res* 113: 151-160, 2003.

Received March 5, 2011
 Revised April 18, 2011
 Accepted April 19, 2011